

Stationary phase evaluation of the integral for the acoustic field around a conical seamount

Michael J. Buckingham

Radio and Navigation Department, Royal Aircraft Establishment, Farnborough, Hampshire, GU14 6TD, England and Institute of Sound and Vibration Research, The University, Southampton, SO9 5NH, England

S. A. S. Jones and Peter N. Harriman

Radio and Navigation Department, Royal Aircraft Establishment, Farnborough, Hampshire, GU14 6TD, England

(Received 14 November 1985; accepted for publication 17 March 1986)

An expression derived recently for the acoustic field from a point source in the channel around a conical seamount involves an integral with a highly oscillatory integrand. This integral is examined here and evaluated using the method of stationary phase. A relatively simple approximate expression for the spatial dependence of the field is obtained whose detailed properties compare very favorably with those of the original formulation.

PACS numbers: 43.30.Bp, 43.30.Es, 43.20.Bi, 92.10.Vz

INTRODUCTION

In a recent theoretical analysis, Buckingham¹ derived an expression for the acoustic field from a point source in an ocean channel surrounding a conical seamount. The geometry he considered was such that the apex of the cone representing the seamount just touches the surface of the ocean, and the point of intersection was made the origin of the spherical polar coordinate system used in the analysis. His result for the velocity potential (excluding the harmonic time dependence) is the following sum of normal modes:

$$\Phi = \frac{2Q}{\alpha_0 \pi \sqrt{\cos \alpha \cos \alpha'}} \sum_{m=1}^{\infty} A_m(r, r', \phi) \times \sin \left[\left(m - \frac{1}{2} \right) \frac{\pi \alpha}{\alpha_0} \right] \sin \left[\left(m - \frac{1}{2} \right) \frac{\pi \alpha'}{\alpha_0} \right], \quad (1)$$

where Q is the source strength, α_0 is the channel angle, r and r' are the ranges of the receiver and source, respectively, measured from the apex, α and α' are the angular depths of the receiver and source, respectively, measured from the sea surface, and ϕ is the azimuthal direction of the receiver measured from the source. The (complex) mode amplitude function A_m is given by the following expression:

$$A_m(r, r', \phi) = \frac{j\pi}{2\sqrt{rr'}} \left(H_0^{(1)}(kR_\phi) - kr_{cm} \int_{|\phi|}^{\pi} \frac{w}{\sqrt{w^2 - \phi^2}} \times H_0^{(1)}(kR_w) J_1(kr_{cm} \sqrt{w^2 - \phi^2}) dw \right), \quad (2)$$

where $H_0^{(1)}(\)$ is the Hankel function of the first kind of zero order, $J_1(\)$ is the Bessel function of the first kind of order unity, r_{cm} is the cutoff range of the m th mode measured from the apex, k is the wavenumber, and

$$\begin{aligned} R_x &= R_0 \sqrt{1 - 2a \cos x}, \\ R_0 &= \sqrt{r^2 + r'^2}, \\ a &= rr'/R_0^2. \end{aligned} \quad (3)$$

The expression for A_m in Eq. (2) was evaluated numerically in Ref. 1. The result shows that the energy in each mode

is spread part of the way around the seamount, and that a shadow zone is formed at the rear of the structure. A simple expression for the angular width of the shadow was derived in Ref. 1 from arguments concerning the stationary points in the argument of the highly oscillatory integrand in Eq. (2). The stationary phase method is pursued below, where it is used to derive an approximate expression for the integral in Eq. (2). This relatively simple expression is a very good representation of the field in the ensonified region of each mode. It shows rapid spatial oscillations similar to those obtained from the numerical evaluation of Eq. (2), and it cuts off at the shadow edge in good agreement with the computed field.

I. STATIONARY PHASE EVALUATION

We let the integral in Eq. (2) be

$$I = \int_{|\phi|}^{\pi} \frac{w}{\sqrt{w^2 - \phi^2}} H_0^{(1)}(kR_w) J_1(kr_{cm} \sqrt{w^2 - \phi^2}) dw. \quad (4)$$

Now, for frequencies of interest in many applications, the argument of the Hankel function in the integrand of I is much greater than unity [provided $r \neq r'$ and $\phi \neq 0$, which is not a serious restriction, since it is merely the condition for the integral in Eq. (2) to be dominant compared with the Hankel function term]. Similarly, the argument of the Bessel function is much greater than unity over most of the integration range away from the lower limit $|\phi|$. Anticipating that contributions to the integral are negligible from the region of the lower limit, we approximate the Hankel and Bessel functions by their asymptotic forms:

$$H_0^{(1)}(kR_w) \simeq \sqrt{2/\pi k R_w} \exp[j(kR_w - (\pi/4))] \quad (5a)$$

and

$$\begin{aligned} J_1(kr_{cm} \sqrt{w^2 - \phi^2}) &\simeq \sqrt{2/[\pi kr_{cm} (w^2 - \phi^2)^{1/2}]} \\ &\times \cos(kr_{cm} \sqrt{w^2 - \phi^2} - 3\pi/4). \end{aligned} \quad (5b)$$

These are highly oscillatory functions which, when substituted into Eq. (4), allow the integral I to be expressed as

$$I = -(1/\pi k \sqrt{r_{cm}})(I_+ - jI_-), \quad (6)$$

where

$$I_{\pm} = \int_{|\phi|}^{\pi} \frac{w}{R_w^{1/2}(w^2 - \phi^2)^{3/4}} \times \exp jk(R_w \pm r_{cm}\sqrt{w^2 - \phi^2}) dw. \quad (7)$$

This integral can be reduced still further by expanding R_w in a Taylor series:

$$R_w = R_0(1 - 2a \cos w)^{1/2} = R_0(1 - a \cos w + \dots), \quad (8)$$

which gives

$$I_{\pm} \simeq \exp(jkR_0) \int_{|\phi|}^{\pi} g(w) \exp -jk\rho U_{\mp} dw, \quad (9)$$

where

$$U_{\mp} \equiv U_{\mp}(w) = \cos w \mp (r_{cm}/\rho)(w^2 - \phi^2)^{1/2} \quad (10)$$

and

$$\rho = R_0 a = \frac{r r'}{\sqrt{r^2 + r'^2}} \simeq \begin{cases} r', & \text{when } r \gg r', \\ r, & \text{when } r' \gg r. \end{cases} \quad (11)$$

The function $g(w)$ in Eq. (9) is

$$g(w) = \frac{w}{R_w^{1/2}(w^2 - \phi^2)^{3/4}}, \quad (12)$$

which, for $w > |\phi|$, is slowly varying compared with the exponential function in the integrand of Eq. (9).

Integrals of the type shown in Eq. (9) can be evaluated using the method of stationary phase.² This is based on the idea that, for $k\rho \gg 1$ (which is our case), the major contributions to the integral come from regions where the function U_{\mp} passes through stationary points. Now, these stationary points are found by differentiating U_{\mp} with respect to w and setting the result equal to zero:

$$\left. \frac{dU_{\mp}}{dw} \right|_{w=\bar{w}} = -\sin \bar{w} \mp \left(\frac{r_{cm}}{\rho} \right) \frac{\bar{w}}{(\bar{w}^2 - \phi^2)^{1/2}} = 0, \quad (13)$$

where \bar{w} is the value of w at a turning point. On examining Eq. (13), and observing that \bar{w} must lie within the interval $[|\phi|, \pi]$ corresponding to the integration range in Eq. (9), we see that U_{-} has no stationary point within the range of integration. Therefore, the contribution from I_{+} to the integral I in Eq. (6) is negligible, allowing us to write

$$I \simeq (j/\pi k \sqrt{r_{cm}}) I_{-}. \quad (14)$$

To evaluate the integral I_{-} , we must look for stationary points in the function U_{+} . These are the solutions of the equation

$$\left. \frac{dU_{+}}{dw} \right|_{w=\bar{w}} = -\sin \bar{w} + \left(\frac{r_{cm}}{\rho} \right) \frac{\bar{w}}{(\bar{w}^2 - \phi^2)^{1/2}} = 0, \quad (15a)$$

that is, we have to solve the transcendental equation

$$\sin \bar{w} = (r_{cm}/\rho) [\bar{w}/(\bar{w}^2 - \phi^2)^{1/2}] \quad (15b)$$

for the roots \bar{w} . The functions on either side of this equation are sketched in Fig. 1 for three different values of $|\phi|$. For the case shown in Fig. 1(a), there are clearly no real roots of Eq. (15b) because $|\phi|$ is greater than some critical value corresponding to the shadow edge. An approximate expression

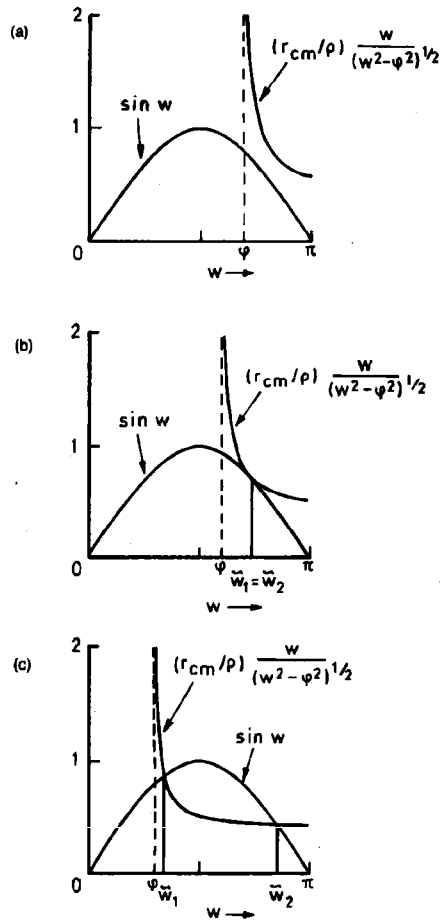


FIG. 1. Sketches of the functions in Eq. (15b) for the three different values of ϕ indicated by the vertical broken lines ($r_{cm}/\rho = 0.42$). (a) ϕ in the shadow zone, no real roots; (b) ϕ at the shadow edge, one real root $w = \bar{w}_1 = \bar{w}_2$; (c) ϕ in the ensonified region, two real roots at the crossover points $w = \bar{w}_1$ and $w = \bar{w}_2$.

for the critical value is derived in Ref. 1. At the shadow edge [Fig. 1(b)] the two curves just touch, and Eq. (15b) has a single real root. For values of $|\phi|$ less than the critical value, the two curves cross [Fig. 1(c)] and Eq. (15b) has two real roots, which fall at the crossover points where $w = \bar{w}_1$ and $w = \bar{w}_2$. Thus the only sensible nonzero values of I_{-} occur when $|\phi|$ is less than or equal to the critical value, that is to say, in the ensonified region of the mode.

The roots of Eq. (15b) can be expressed in the form

$$\bar{w} = f(\phi), \quad (16)$$

where $f(\phi)$ is a double-valued function of ϕ , as shown in the sketch in Fig. 2. The two branches of the function meet when $|\phi|$ equals the critical value, at the shadow edge. For smaller values of $|\phi|$, in the ensonified region, the two roots of Eq. (15b) are associated with the lower and upper branches, as shown in the diagram. In practice, these roots may be evaluated using a simple numerical technique implemented on a digital computer. The turning point occurring at $w = \bar{w}_1$ (lower branch) is a maximum and that at $w = \bar{w}_2$ (upper branch) is a minimum.

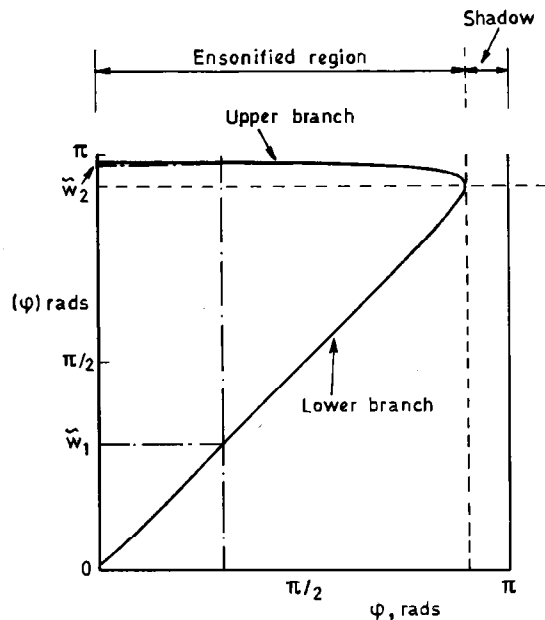


FIG. 2. Sketch of the function $f(\phi)$ showing its double-valued nature ($r_{cm}/\rho = 0.06$). For a given value of ϕ the two roots are \tilde{w}_1 and \tilde{w}_2 , associated with the lower and upper branches, respectively, as shown here.

Assuming then that the stationary points of U_+ (i.e., \tilde{w}_1 and \tilde{w}_2) are known, it is a straightforward matter to evaluate I_- using the stationary phase approximation. The standard stationary phase result² gives

$$I_- = \sqrt{\frac{2\pi}{k\rho}} \exp(jkR_0) \times \left(\frac{g(\tilde{w}_1)}{|U_+''(\tilde{w}_1)|^{1/2}} e^{-j[k\rho U_+(\tilde{w}_1) - (\pi/4)]} + \frac{g(\tilde{w}_2)}{|U_+''(\tilde{w}_2)|^{1/2}} e^{-j[k\rho U_+(\tilde{w}_2) + (\pi/4)]} \right), \quad (17)$$

where $U_+''(\tilde{w})$ is the second derivative of U_+ evaluated at the stationary point $w = \tilde{w}$:

$$U_+''(\tilde{w}) = \frac{d^2 U_+}{d\tilde{w}^2} \Big|_{\tilde{w}=\tilde{w}} = -\cos \tilde{w} - \left(\frac{r_{cm}}{\rho} \right) \frac{\phi^2}{(\tilde{w}^2 - \phi^2)^{3/2}}. \quad (18)$$

The expression for the mode amplitude function in Eq. (2) can now be written as

$$A_m(r, r', \phi) = (j\pi/2\sqrt{rr'}) [H_0^{(1)}(kR_\phi) - kr_{cm}I] \approx \sqrt{(r_{cm}/4rr')} I_- \approx \sqrt{(\pi r_{cm}/2rr'k\rho)} \exp(jkR_0) \times \left(\frac{g(\tilde{w}_1)}{|U_+''(\tilde{w}_1)|^{1/2}} e^{-j[k\rho U_+(\tilde{w}_1) - (\pi/4)]} + \frac{g(\tilde{w}_2)}{|U_+''(\tilde{w}_2)|^{1/2}} e^{-j[k\rho U_+(\tilde{w}_2) + (\pi/4)]} \right), \quad (19)$$

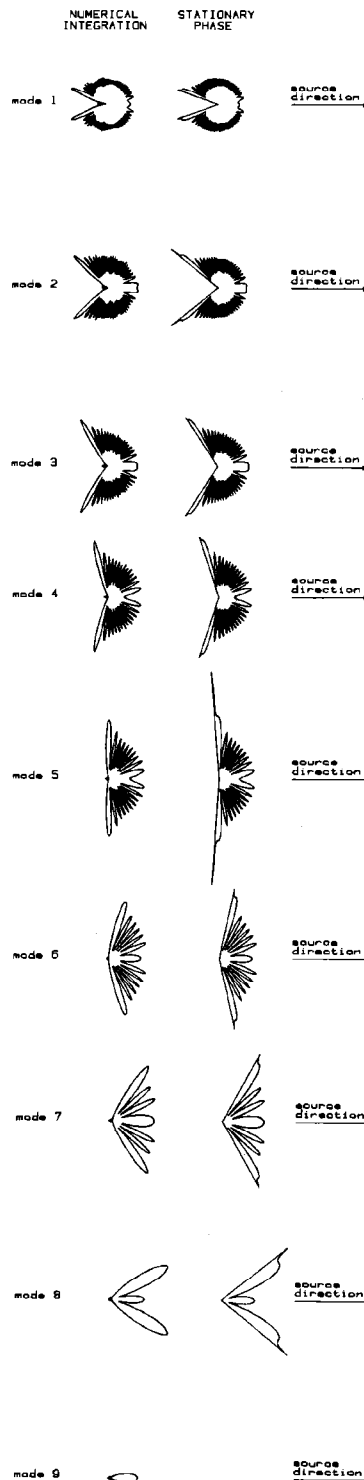


FIG. 3. Comparison of the azimuthal mode shapes, as calculated from Eq. (2) (left) and the stationary phase result in Eq. (20) (right). Here, $kr = 100$, $kr' = 10^4$, $\alpha_0 = \pi/12$.

where the contribution from the Hankel function has been neglected since this is insignificant except in the immediate vicinity of the source.¹ It follows from Eq. (18) that the modulus of A_m is

$$|A_m| \approx \sqrt{\frac{\pi r_{cm}}{2rr'k\rho} \left(\frac{g^2(\tilde{w}_1)}{|U''_+(\tilde{w}_1)|} + \frac{g^2(\tilde{w}_2)}{|U''_+(\tilde{w}_2)|} + \frac{2g(\tilde{w}_1)g(\tilde{w}_2)}{|U''_+(\tilde{w}_1)|^{1/2}|U''_+(\tilde{w}_2)|^{1/2}} \right) \times \sin\{k\rho[U_+(\tilde{w}_1) - U_+(\tilde{w}_2)]\}}^{1/2}. \quad (20)$$

The first two terms in parentheses are slowly varying functions of position (range and azimuth). The third term, involving the high-frequency sine function, represents a rapidly oscillating component of the field which is superimposed on the smoothly varying background level. The spatial oscillations, occurring as a result of interference within the mode, are a direct consequence of horizontal refraction: Acoustic rays following curved trajectories in the horizontal, due to repeated reflections from the boundaries of the channel, cross paths and mutually interfere.¹

ly, there is good agreement between the two sets of curves. For a given mode, both curves show the same number of peaks, which appear at the same angular positions; field cut-off at the shadow edge shows a close correspondence in the two cases; the overall shapes of the two sets of diagrams are very similar. In the lower order modes, the envelopes of the numerically evaluated curves show a slight variation which is absent from their stationary phase counterparts, and at the edge of the shadow zone a spike appears in the stationary phase curves, indicating the breakdown of the approximation as the transition is made from the ensonified region to the shadow. Apart from these very minor discrepancies, the stationary phase results faithfully replicate the numerically evaluated curves, including all the fine structure. The only exception to this is the ninth mode, which is almost but not entirely devoid of energy according to the numerical integration, but which is completely cut off in the stationary phase approximation.